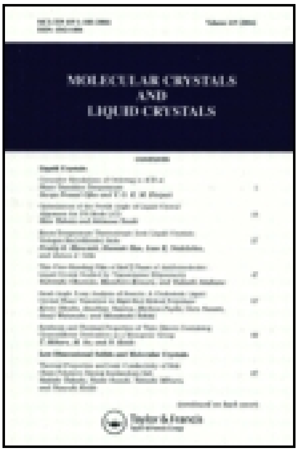

Molecular Crystals and Liquid Crystals
Publication details, including instructions for authors and subscription information:
http://www.tandfonline.com/loi/gmcl20

Temperature-Responsive Bending of Nematic Elastomers with Hybrid Molecular Alignment

Sawa Yoshiki [a], Kenji Urayama [a] & Toshikazu Takigawa [a]
[a] Department of Materials Chemistry, Kyoto University, Kyoto, 615-8510, Japan

To cite this article: Sawa Yoshiki, Kenji Urayama & Toshikazu Takigawa (2011): Temperature-Responsive Bending of Nematic Elastomers with Hybrid Molecular Alignment, Molecular Crystals and Liquid Crystals, 549:1, 106-112

To link to this article: http://dx.doi.org/10.1080/15421406.2011.581157

Mol. Cryst. Liq. Cryst., Vol. 549: pp. 106–112, 2011
Copyright © Taylor & Francis Group, LLC
ISSN: 1542-1406 print/1563-5287 online
DOI: 10.1080/15421406.2011.581157

Temperature-Responsive Bending of Nematic Elastomers with Hybrid Molecular Alignment

SAWA YOSHIKI, KENJI URAYAMA,*
AND TOSHIKAZU TAKIGAWA

Department of Materials Chemistry, Kyoto University, Kyoto 615-8510, Japan

*We demonstrate thermally induced giant bending of nematic elastomer films with hybrid alignment (HNEs) where the director continuously rotates by 90° (from planar alignment to vertical alignment) between the top and bottom surfaces. In the nematic state, a thermally induced change in local nematic order results in a markedly temperature (*T*) dependent curvature of HNEs including the reversal of bending direction. In the high-temperature isotropic state, the curvature is* T*-independent. This bending deformation is thermally reversible. The* T *dependence of curvature is well explained by a simple elastic model assuming a linear variation of strain in the thickenss direction with the thermomechanical data of the corresponding nematic elastomers with globally planar or vertical alignment. The* T*-responsive bending feature of the HNEs has potential application as soft solid sensors that behave like bimetals.*

1. Introduction

Liquid crystal elastomers (LCEs) are an interesting hybrid material of liquid crystals and rubbers. A unique feature of LCEs is the strong coupling of macroscopic shape and molecular orientation. This feature produces a rich variety of stimulus-responsive behavior.[1–3] A fascinating responsive property is thermally induced large deformation. A change in orientational order caused by temperature variation leads to a finite macroscopic strain. A simple uniaxial nematic alignment drives a uniaxial deformation of LCEs: The LCEs elongate and contract uniaxially with cooling and heating, respectively.[4–7]

Complicated deformation modes such as bending and twisting are possible by introducing the corresponding types of nonuniform director configuration into the LCEs. In fact, several researtures showed a finite gradient of nematic order along the thickness direction caused by light irradiation[8–11] or temperature gradient[12] leads to a large bending of the highly-cross-linked LC films or LCE films. Broer et al.[13] demonstrated thermally driven bending of a highly-cross-linked LC film that inherently has hybrid mesogen alignment where the director continuously rotates by 90° (from planar alignment to vertical alignment) between top and bottom surfaces of the film. Their film was substantially glassy not elastomeric because of the high cross-link concentration, which was obvious from the high elastic modulus on the order of gigapascals. This was because their purpose was to enhance the force generated by curling. In their case, the curling primarily results from a gradient of thermal expansion coefficient in the thickness direction due to anisotropic orientation, rather than a temperature change in local nematic order. In present study, we demonstrate

---

*Corresponding author. E-mail: urayama@rheogate.polym.kyoto-u.ac.jp

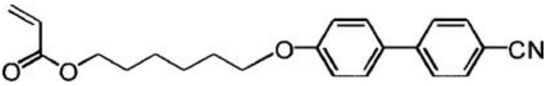

Figure 1. Employed monoacrylate mesogen.

a temperature change in local nematic order in the elastomeric films with hybrid alignment (HNEs) induces considerably larger bending. The temperature-responsive bending property of the HNEs has potential application as soft solid sensors that behave like bimetals.

2. Experimental Section

The details of the prepration of the HNE films were described elsewhere.[14] The side-chain-type HNE films were prepared by the photopolymerization of the monoacrylate mesogenic monomer (A-6OCB; Figure 1) and 1,6-hexanediol diacrylate (cross-linker) using bis(cyclopentadienyl)bis[2,6-difluoro-3-(-pyrryl)phenyl]titanium (Irgacure 784) as a photoinitiator. A-6OCB was mixed with a miscible nonreactive mesogenic solvent 4-n-hexyloxy-4′-cyanobiphenyl 6OCB (A-6OCB:6OCB = 5:4 by weight ratio) to broaden the temperature range of the nematic phase. The cross-linker concentration was 7 mol% in feed. The photopolymerization was conducted in a glass cell with a cell gap of 42 or 97 μm by the irradiation of the light of a wavelength 526 nm at 313 K in the nematic state. The surfaces of the upper and bottom substrates were coated with different types of polyimide layer to induce planar and vertical mesogen alignment, respectively. After the irradiation, the resulting gel films were detached from the substrates by immersing the cell in dichloromethane. The detached films were allowed to swell in dichloromethane to wash out the unreacted materials and nonreactive solvent. The swollen films were gradually deswollen by increasing the methanol content in the swelling solvent, and the HNE films were obtained by drying the deswollen gels in air. Although this deswelling process induced a curling, the films became flat at a certain temperature (T_{flat}), which will be shown later. At T_{flat}, the rectangular specimens were cut out from the sheet so that one dimension could be parallel to the rubbing axis of the polyimide layer. The dimensions of the rectangular specimens were ca. 2.5 mm in length and ca. 0.5 mm in width. The thickness of the two HNE films (HNE-36 and HNE-83) in the dry state was 36 μm and 83 μm, respectively, each of which was measured at T_{flat}. The nematic-isotropic transition temperautures (T_{NI}) of HNE-36 and HNE-83 were 363 K and 361 K, respectively.

The thermal deformation of the dry HNEs was observed with an optical microscope equipped with CCD camera using the geometry shown in Figure 2a. One end of the specimen was attached to a Teflon® plate, and it was immersed in a temperature controllable bath of a silicone oil that was a nonsolvent for the specimen. The fixed end part was sufficiently small so that the effect on the bending deformation of the film could be negligible. The radius of the curvature (r) in the equilibrium state at each temperature was evaluated by video analysis, i.e., by superposing a circle with a radius of r on the outline of the specimen.

3. Results and Discussion

Figure 3 shows the optical micrographs of the shape of HNE-36 at various temperatures. The film considerably curls at $T = 368$ K in the high-temperature isotropic state. In the T

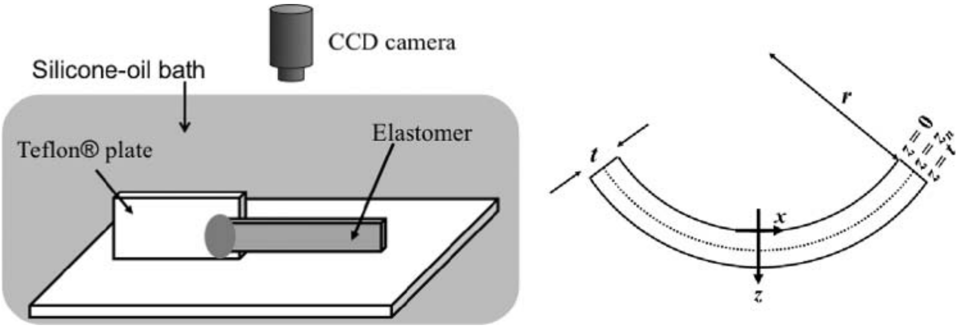

Figure 2. (a) Observation geometry for bending deformation. (b) Film with a curvature of $1/r$ and a thickness of t. The neutral plane with zero strain corresponds to $z = z_n$.

regime of isotropic state, the shape is T-independent. When the cooling drives the isotropic-to-nematic transition, the curling starts to become small. The curling becomes totally absent and the film becomes flat at a certain temperature (T_{flat}) around 338 K. Further cooling induces a curling in the opposite direction, and the degree of bending increases with cooling. HNE-83 exhibits the similar behavior, and the movie of the thermal bending distortion is available in the supporting information of Ref.14.

Figure 4a shows the curvature $1/r$ as a function of T for HNE-36 and HNE-83. For the sake of convenience, the curvatures at the high and low T are defined to be positive and negative, respectively, because the curling direction changes at T_{flat}. The strongly T-dependent curvature is observed in the nematic state, while the curvature is T-indepdendent in the isotropic state. The deformation behavior is thermally reversible. These results clearly indicate that the bending is driven by a change in local nematic order. The curvature becomes larger as the film thickness (t) decreases, although t has no effect on T_{flat}. The temperature T_{flat} is different from the preparation (cross-linking) temperature ($T_0 = 313$ K). The stage of cross-linking in the presence of solvent (ca. 50 wt%) at T_0 corresponds to the initial flat state with hybrid alignment. The subsequent deswelling to the dry state leads to a bending deformation due to a finite strain gradient caused by anisotropic shrinking. A finite degree of bending in the dry state is observed around T_0 (Figure 4a). Volume change of nematic gels with global director simultaneously induces a considerably anisotropic shape variation.[15, 16] The bending deformation observed here is composed of the two contributions, i.e., anisotropic shrinking due to the deswelling to the dry state, and the change in local nematic order due to temperature variation (Figure 5).

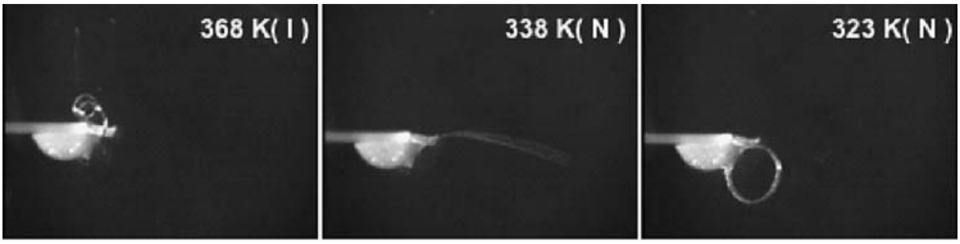

Figure 3. Optical micrographs of the thermal bending deformation for HNE-36.

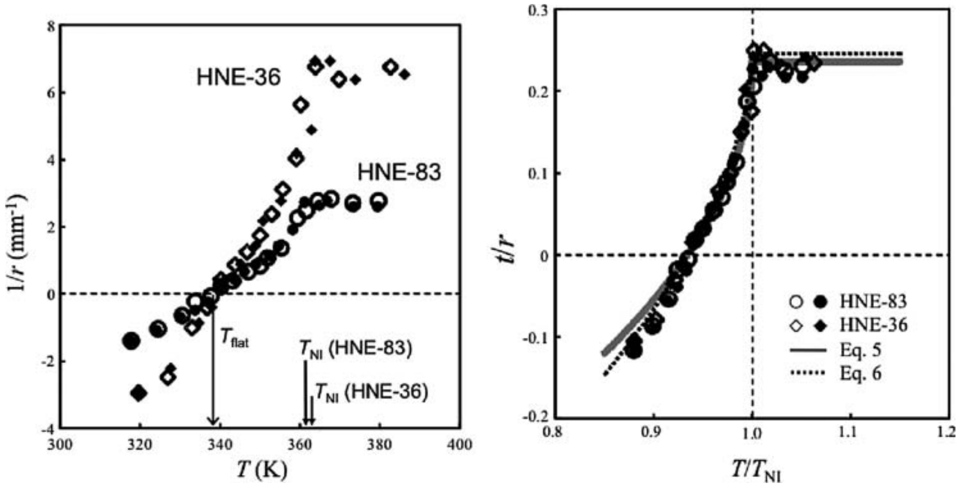

Figure 4. (a) Temperature dependence of the curvature 1/*r* of HNE-36 and HNE-83 in cooling (open symbols) and heating processes (filled symbols). (b) Nomarized temperature dependence of reduced curvature *t/r* for HNE-36 and HNE-83. The solid and dotted lines represent the calculation curves using eqs 5 and 6, respectively. The data are reproduced from Ref.14.

The coefficient d(1/*r*)/d*T* can be a measure of the thermal effect on bending, and it is roughly evaluated to be ca. 2×10^{-1} mm^{-1} K^{-1} for HNE-36. This is about two orders of magnitude larger than that (ca. 1×10^{-3} mm^{-1}K^{-1}) obtained for a highly cross-linked glassy LC film having hybrid alignment with almost the same thickness (40 μm).[13] Their glassy films have a finite gradient of thermal expansion coefficient in the thickness direction, but the local nematic order substantially frozen in the glassy matrix is not sensitive to temperature change. In contrast, the glass transition temperature of the HNEs is around 40°C, and the *T* range examined here is in the rubbery state. The local nematic order in the rubbery matrix is variable in sharp response to temperature variation. The strong coupling between nematic order and strain in the elastomer films boosts a change in the strain gradient driven by temperature variation.

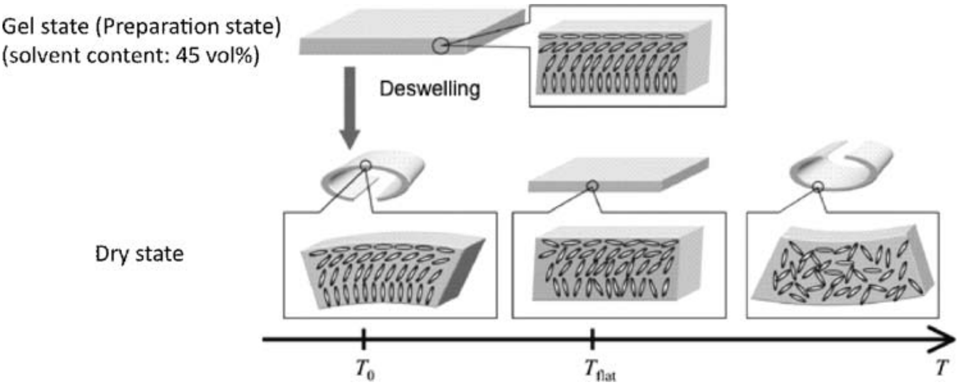

Figure 5. Schematic for the mechanism of bending deformation of HNEs. The bending consists of the contributions of deswelling and temperature change.

The curling originates from a finite gradient of strain (ε_x) in the thickness direction (z-axis). For elastically isotropic materials with sufficiently small thickness ($t \ll r$) (Figure 2b), ε_x is given by

$$\varepsilon_x(z) = \frac{z - z_n}{r + z_n} \approx \frac{z - z_n}{r} \tag{1}$$

where z_n is the position of a neutral plane with $\varepsilon_x = 0$, and ε_x is assumed to vary linearly with the distance from the neutral plane.[12,17] From eq. 1, the reduced curvature (t/r) is simply given by the difference in ε_x at the top and bottom surfaces:

$$\frac{1}{r} = \frac{\varepsilon_x(t) - \varepsilon_x(0)}{t} = \frac{\Delta\varepsilon}{t} \tag{2}$$

This equation correlates the curvature ($1/r$) and the gradient of strain ($\Delta\varepsilon/t$), and it also shows that the curvature increases as the film is thinner if $\Delta\varepsilon$ is the same. Figure 4b shows the T dependence of the reduced curvature (t/r) for HNE-36 and HNE-83. The thickness measured in the flat state ($T_{\mathrm{flat}} = 338$ K) is used as t. The T dependence of t is expected to be small due to the cancellation of the thickening and thinning effects on the film thickness. The reduced curves for the films with different t collapse into a single curve in agreement with eq. 2.

The direct measurements of $\varepsilon_x(t)$ and $\varepsilon_x(0)$ in HNEs are difficult. Alternatively, the strains of the nematic elastomers with globally planar and vertical alignments (PNE and VNE, respectively) may be applicable to $\varepsilon_x(t)$ and $\varepsilon_x(0)$. Figure 6 shows the T effect of the principal ratios λ_i ($i = \parallel, \perp$) in the directions parallel and normal to the director for PNE and VNE both of which have the same cross-link concentration (7 mol% in feed) as the HNEs. The ratio λ_i is defined by $\lambda_i = l_i / l_{i,\mathrm{iso}}$ where l_i and $l_{i,\mathrm{iso}}$ are the dimensions along the i-axis in the state of interest and high-temperature isotropic state, respectively. The superscripts P and V denote PNE and VNE, respectively. As in the cases of many earlier studies, PNE and VNE exhibit uniaxial elongation along the director in the cooling in the

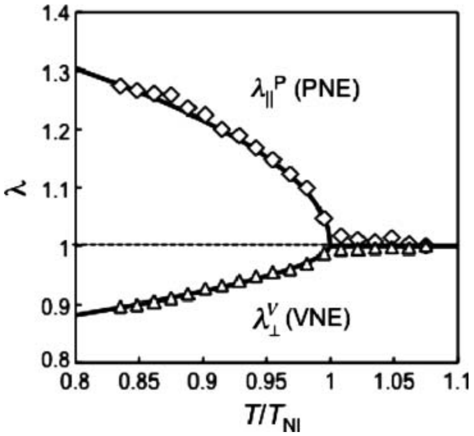

Figure 6. Temperature dependence of principal ratio along the director for the nematic elastomer with globally planar alignment $\lambda_\parallel{}^P$ and that normal to the director of the nematic elastomer with globally vertical alignment $\lambda_\perp{}^V$. The film thickness of PNE and VNE is 30 and 29 μm, respectively. The solid lines represent the fitted results of eq. 3 with the parameter values of a and β. The data are reproduced from Ref.14.

nematic state. The contraction in the direction normal to the director for VNE ($\lambda_\perp{}^V < 1$) indicates the elongation along the director ($\lambda_\parallel{}^V > 1$) due to volume conservation ($\lambda_\parallel \lambda_\perp{}^2 = 1$), although $\lambda_\parallel{}^V$ was not directly measured. The following phenomenological equation[12] was employed to express the T dependence of $\lambda_\parallel{}^P$ and $\lambda_\perp{}^V$:

$$\lambda(Q) = 1 + \beta(1 - Q)^a \tag{3}$$

with $Q = T/T_{NI}$. The fitted values are $a = 0.50$ and $\beta = 0.68$ for $\lambda_\parallel{}^P$ and $a = 0.60$ and $\beta = -0.31$ for $\lambda_\perp{}^V$. The strain γ_i ($i = \parallel, \perp$) is defined so that γ_i can be zero at $Q = Q_{flat}$, i.e., the reference state for the strain is taken at $Q = Q_{flat}$:

$$\gamma_i(Q) = \frac{\lambda_i(Q)}{\lambda_i(Q_{flat})} - 1 \tag{4}$$

If $\varepsilon_x(t)$ and $\varepsilon_x(0)$ in HNEs are approximated by $\gamma_\parallel{}^P$ and $\gamma_\perp{}^V$, respectively, eq. 2 becomes

$$\frac{1}{r(Q)} = \frac{\gamma_\parallel^P(Q) - \gamma_\perp^V(Q)}{t} \tag{5}$$

As can be seen in Figure 4b, the results calculated by eq. 5 (solid line) well agree with the experimental data. The dotted curves were obtained by an alternative approximation where the strains in eq. 2 are replaced by $\gamma_\parallel{}^P$ and $\gamma_\perp{}^P$ where $\gamma_\perp{}^P$ is given by $\gamma_\perp{}^P = (\lambda_\parallel{}^P)^{-1/2} - 1$ assuming the volume conservation:

$$\frac{1}{r(Q)} = \frac{\gamma_\parallel^P(Q) - \gamma_\perp^P(Q)}{t} \tag{6}$$

The dotted curve more satisfactorily describes the data in the nematic state than the solid line. The successful description by eqs 5 or 6 indicates that the strains at the top and bottom surfaces in HNEs are close to those in PNE or VNE, and that the strain distribution in the thickness direction is well approximated by a linear function of z. These results show that thermally induced bending behavior of the HNE films can be predicted with high accuracy by eq. 5 or eq. 6 with the themomechanical data of the corresponding PNE and VNE. A more detailed theory and simulation reveal accurate strain distribution and the strains at the two surfaces of HNEs, and the simulation results support the validity of the approximations used here.[14]

4. Summary

The nematic elastomer films with hybrid alignment along the thickness direction (HNEs) exhibited markedly T-dependent bending including the reversal of the bending direction. A change in local nematic order caused by T variation significantly affects the strain gradient along the thickness direction. The T dependence of the curvature for the HNEs is predicted with high accuracy by a simple elastic bending model with the thermomechanical data of the corresponding nematic elastomers with globally planar or vertical alignment. The T-responsive bending feature of the HNEs has potential application as soft solid sensors with a function like bimetals.

Acknowledgments

This work was partly supported by the Grant-in-Aid on Priority Area "Soft Matter Physics" (No.21015014) and that for Scientific Research (B) (No. 16750186) from the Ministry of Education, Culture, Sports, Science and Technology (MEXT) of Japan.

References

[1] M. Warner and E.M. Terentjev, *Liquid Crystals Elastomers (Revised Edition)* (London: Clarendon Press, 2007).

[2] K. Urayama, "Selected issues in liquid crystal elastomers and gels," *Macromolecules*, **40**, 2277–88 (2007).

[3] C. Ohm, M. Brehmer and R. Zentel, "Liquid Crystalline Elastomers as Actuators and Sensors," *Adv. Mater.*, **22**, 3366–87 (2010).

[4] J. Kupfer and H. Finkelmann, "Nematic Liquid Single-Crystal Elastomers," *Makromol. Chem. Rapid Commun.*, **12**, 717–26 (1991).

[5] S.M. Clarke, A. Hotta, A.R. Tajbakhsh and E.M. Terentjev, "Effect of cross-linker geometry on equilibrium thermal and mechanical properties of nematic elastomers," *Phys. Rev. E*, **64**, 061702 (2001).

[6] H. Wermter and H. Finkelmann, "Liquid Crystalline Elastomers as Artificial Muscles," *e-Polymers*, no. **013** (2001).

[7] D.L. Thomsen, P. Keller, J. Naciri, R. Pink, H. Jeon, D. Shenoy and B.R. Ratna, "Liquid crystal elastomers with mechanical properties of a muscle," *Macromolecules*, **34**, 5868–75 (2001).

[8] Y.L. Yu, M. Nakano and T. Ikeda, "Directed bending of a polymer film by light - Miniaturizing a simple photomechanical system could expand its range of applications," *Nature*, **425**, 145–45 (2003).

[9] M. Camacho-Lopez, H. Finkelmann, P. Palffy-Muhoray and M. Shelley, "Fast liquid-crystal elastomer swims into the dark," *Nat. Mater.*, **3**, 307–10 (2004).

[10] N. Tabiryan, S. Serak, X.M. Dai and T. Bunning, "Polymer film with optically controlled form and actuation," *Opt. Exp.*, **13**, 7442–48 (2005).

[11] C.L. van Oosten, D. Corbett, D. Davies, M. Warner, C.W.M. Bastiaansen and D.J. Broer, "Bending Dynamics and Directionality Reversal in Liquid Crystal Network Photoactuators," *Macromolecules*, **41**, 8592–96 (2008).

[12] K.K. Hon, D. Corbett and E.M. Terentjev, "Thermal diffusion and bending kinetics in nematic elastomer cantilever," *Eur. Phys. J. E*, **25**, 83–89 (2008).

[13] G.N. Mol, K.D. Harris, C.W.M. Bastiaansen and D.J. Broer, "Thermo-mechanical responses of liquid-crystal networks with a splayed molecular organization," *Adv. Funct. Mater.*, **15**, 1155–59 (2005).

[14] Y. Sawa, K. Urayama, T. Takigawa, A. DeSimone and L. Teresi, "Thermally Driven Giant Bending of Liquid Crystal Elastomer Films with Hybrid Alignment," *Macromolecules*, **43**, 4362–69 (2010).

[15] K. Urayama, Y.O. Arai and T. Takigawa, "Anisotropic swelling and phase behavior of monodomain nematic networks in nematogenic solvents," *Macromolecules*, **38**, 5721–28 (2005).

[16] K. Urayama, Y.O. Arai and T. Takigawa, "Volume phase transition of monodomain nematic polymer networks in isotropic solvents accompanied by anisotropic shape variation," *Macromolecules*, **38**, 3469–74 (2005).

[17] M. Warner and L. Mahadevan, "Photoinduced deformations of beams, plates, and films," *Phys. Rev. Lett.*, **92**, 134302 (2004).